Front. Optoelectron. 2015, 8(2): 170–176
DOI 10.1007/s12200-015-0480-4

RESEARCH ARTICLE

Vascular distribution imaging of dorsal skin window chamber in mouse with spectral domain optical coherence tomography

Jian GAO[1], Xiao PENG[1], Peng LI (✉)[2], Zhihua DING[2], Junle QU[1], Hanben NIU[1]

1 Key Laboratory of Optoelectronic Devices and Systems of Ministry of Education and Guangdong Province, College of Optoelectronic Engineering, Shenzhen University, Shenzhen 518060, China

2 State Key Laboratory of Modern Optical Instrumentation, Department of Optical Engineering, Zhejiang University, Hangzhou 310027, China

Abstract Doppler optical coherence tomography or optical Doppler tomography (ODT) has been demonstrated to spatially localize flow velocity mapping as well as to obtain images of microstructure of samples simultaneously. In recent decades, spectral domain Doppler optical coherence tomography (OCT) has been applied to observe three-dimensional (3D) vascular distribution. In this study, we developed a spectral domain optical coherence tomography system (SD-OCT) using super luminescent diode (SLD) as light source. The center wavelength of SLD is 835 nm with a 45-nm bandwidth. Theoretically, the transverse resolution, axial resolution and penetration depth of this SD-OCT system are 6.13 μm, 6.84 μm and 3.62 mm, respectively. By imaging mouse model with dorsal skin window chamber, we obtained a series of real-time OCT images and reconstructed 3D images of the specific area inside the dorsal skin window chamber by Amira. As a result, we can obtain the clear and complex distribution images of blood vessels of mouse model.

Keywords optical coherence tomography (OCT), mouse, dorsal skin window chamber, vascular distribution

1 Introduction

Optical coherence tomography (OCT) is a non-invasive and non-destructive optical imaging technology, first proposed by Huang et al. in 1991 [1]. Compared with X-Ray, ultrasound and magnetic resonance imaging, OCT is called "optical biopsy" [2], because of its specific advantages such as high resolution, high sensitivity and real-time imaging. In 1991, Huang et al. obtained the microstructure of human retina and the structure of coronary artery wall successfully by building a time-domain optical coherence tomography (TD-OCT) system [1]. However, in this method, the length of the reference arm is rapidly scanned over a distance that corresponds to the imaging-depth range of the sample, leading to limited imaging speed. Fourier-domain OCT (FD-OCT), which has high signal-to-noise ratio (SNR) and high sensitivity, was later developed [3–5].The depth information of the sample is not obtained by mechanical scanning of the reference arm but by Fourier transform based on the detected spectral signal. According to the difference of probing scheme, FD-OCT can be divided into two types, spectral domain OCT [6] and swept source OCT [7,8]. So far, research groups have made great efforts to improve OCT by developing various functional expansions of traditional OCT, such as Doppler OCT [9], polarization-sensitive OCT [10] and molecular contrast OCT [11]. These developments have made OCT technology widely applied in biomedicine [12–18], particularly in ophthalmology [19]. Doppler OCT can obtain high-resolution images of tissue structure and hemodynamics simultaneously, combining Doppler effect with OCT technology. Doppler OCT has been applied to the depth-resolved cross-sectional flow imaging of tissues *in vivo* [20–24]. Furthermore, blood flow imaging of retina vessels was also achieved by Doppler OCT [25,26]. These results were based on TD-OCT system, in which mechanical scanning of the reference arm exists. Compared with TD-OCT, spectral domain optical coherence tomography system (SD-OCT) has higher sensitivity [3,4] and the imaging speed is 150 times faster than TD-OCT [27].Therefore, researchers have focused on using FD-OCT system to observe blood flow imaging of retina vessels [28–30].

Received September 26, 2014; accepted January 20, 2015

E-mail: peng_li@zju.edu.cn, jlqu70@gmail.com

Wang's group and Yatagai's group have done a lot of research on three-dimensional (3D) visualization of retinal vessels. They developed high-speed SD-OCT system to gain 3D images of the blood vessels in mouse brain, i.e., optical coherence angiography (OCA) [31,32]. Vakoc et al. applied optical frequency domain imaging (OFDI) technology to detect the microenvironment of various tumor models at varying sites in mice, gaining 3D depth-projected vascular distribution of brain bearing tumor and cross-sectional images of back implanted in the dorsal skin fold chamber model with an MCaIV tumor [33]. However, high-resolution, 3D vascular distribution of the mouse with dorsal skin window chamber has not been obtained by SD-OCT system till now. Here, the mentioned chamber implanted into the dorsal skin in mice [34] was derived from Sandison [35] in order to investigate the microcirculation. Because of repeated analysis of the microcirculation over a period of time, this animal model has been applied to assess not only the angiogenesis in a variety of processes including endometriosis and tumor growth, but also the early phases of preclinical development of Bevacizumab [36,37].

In this study, we developed an SD-OCT system for imaging mouse model with dorsal skin window chamber, obtained a series of real-time OCT images and reconstructed 3D images of the specific area inside the dorsal skin window chamber mouse.

2 Experimental setup

OCT system is a low coherent system based on Michelson interferometer. The schematic diagram of the system used in this study is shown in Fig. 1.

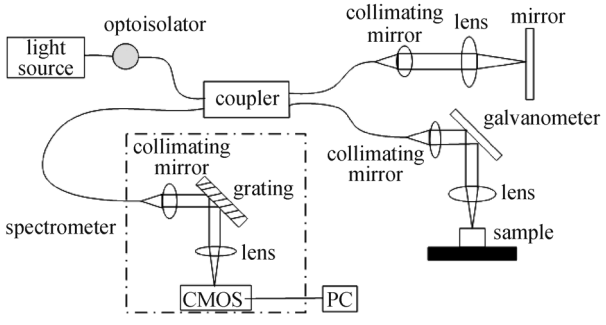

Fig. 1 Schematic diagram of spectral-domain OCT system. CMOS: complementary metal oxide semiconductor; PC: personal computer

The low-coherence light emitted from the broadband light source enters the Michelson interferometer through optoisolator. The function of optoisolator is to protect the light source from reflected light. The beam is divided into two parts by a 90/10 coupler via optical fiber and 90% of the beam is guided to the sample arm and focused on the sample after collimating mirror and galvanometer. The light in the reference arm is focused on the mirror after collimating mirror and lens. The high speed interferometer receives interference signal produced by the reflected lights from the sample arm and the reference arm. Finally, the data is processed by computer using home-built software in Labview.

The axial resolution and transverse resolution of the spectral domain OCT is independent of each other. The axial resolution δ_z is decided by coherence length l_c, namely center wavelength and 3 dB bandwidth of the broadband source [38,39]. In the SD-OCT system, we used a super luminescent diode (SLD) (Superlum) with a center wavelength of 835 nm. The full width half maximum (FWHM) of the SLD is 45 nm and the output power is 12 mW. According to these parameters, the axial resolution can be calculated as follows:

$$\delta_z = l_c = \frac{2\ln 2}{\pi} \cdot \frac{\lambda_0^2}{\Delta\lambda} = \frac{2\ln 2}{\pi} \cdot \frac{0.835 \times 0.835}{45 \times 10^{-3}}\ \mu\text{m} \approx 6.84\ \mu\text{m}, \quad (1)$$

where λ_0 and $\Delta\lambda$ are the center wavelength and bandwidth of the SLD, respectively. The output spectrum curve of SLD is shown in Fig. 2.

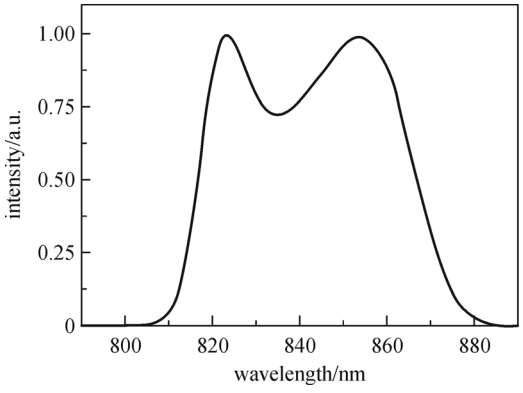

Fig. 2 Output spectrum curve of the optical source

The transverse resolution of the SD-OCT system depends on the objective lens that is to focus the light onto the sample according to Rayleigh criterion. The sample arm consists of a collimating mirror (f_c = 20 mm, OZ optics), scanning galvanometer (6215H, Cambridge Technology) and lens (f_{obj} = 30 mm, DHC). The numerical aperture (NA) of the optical fiber is 0.13. The transverse resolution can be calculated as

$$\Delta x = \frac{4\lambda_0}{\pi} \cdot \frac{f_{obj}}{d} = \frac{4\lambda_0}{\pi} \cdot \frac{f_{obj}}{2\text{NA} \cdot f_c} = \frac{4 \times 0.835}{\pi} \cdot \frac{30}{2 \times 0.13 \times 20}\ \mu\text{m} \approx 6.13\ \mu\text{m}, \quad (2)$$

where d is the diameter of the light spot on the lens of the sample arm.

High speed spectrometer plays an important role in SD-OCT system. The quality of the images depends on the scanning speed of the spectrometer. The high speed spectrometer consists of achromatic collimating lens (f_c = 60 mm, OZ optics), diffraction grating on the condition of Littrow with a center wavelength of 830 nm and line per mm of 1200 (Wasatch Photonics), near infrared achromatic lens (f = 150 mm, TECHSPEC®NearIRdoublets, Edmundoptics) and a 12-bitline-scan CMOS camera with 4096 pixels (Basler sprint, SPL4096-140K). The pixel size and line rate of the CMOS are 10 μm × 10 μm and 140 KHz, respectively. According to the grating equation:

$$d(\sin\theta_0 + \sin\theta) = m\lambda, \tag{3}$$

diffraction angle at center wavelength can be calculated by Eq. (3). In general, m is considered as 1.

$$2d\sin\theta_0 = m\lambda_0.$$

$$\sin\theta_0 = \frac{1 \times 830 \times 10^{-6}}{2 \times (1/1200)} = 0.498,\ \theta_0 \approx 29.87°, \tag{4}$$

where λ_0 and d are center wavelength and line number of the grating, respectively. Spectral resolution of the spectrometer can be obtained based on above parameters. At first, spectral resolution of the grating follows:

$$\begin{aligned}\delta\lambda_g &= \frac{\lambda_0}{mN} = \frac{\lambda_0}{m\left(D/(d\cos\theta_0)\right)} = \frac{\lambda_0 d\cos\theta_0}{mD} \\ &= \frac{835 \times (1/1200) \times \cos 29.87}{1 \times 2 \times 0.13 \times 60}\ \text{nm} \\ &\approx 0.039\ \text{nm}.\end{aligned} \tag{5}$$

Here, N is line number in the spot through collimating mirror on the grating. D is the diameter of the spot, D = 2NA·f_c.

Moreover, spectral resolution decided by pixel size p of line-scan CMOS:

$$\begin{aligned}\delta\lambda_c &= \frac{p}{fm/(d\cos\theta_0)} \\ &= \frac{10 \times 10^3 \times (1/1200) \times \cos 29.87}{1 \times 150}\ \text{nm} \\ &\approx 0.04818\ \text{nm}.\end{aligned} \tag{6}$$

Therefore, the spectral resolution of the high speed spectrometer in our system is 0.04818 nm by comparing Eq. (5) with Eq. (6). According to sampling theorem, theoretically the imaging depth of this SD-OCT system [4,5,40] in air is

$$\begin{aligned}Z_{\max} &= \frac{\lambda_0^2}{4\delta\lambda} = \frac{835 \times 835}{4 \times 0.04818}\ \text{nm} \approx 3.62 \times 10^6\text{nm} \\ &= 3.62\ \text{mm}.\end{aligned} \tag{7}$$

3 Results and discussion

In the experiment, mice are bought from medical laboratory animal center in Guangdong province. The requirements are female BALB/c-nu mice of more than 8 weeks old and > 20 g to be fit for dorsal skin window chamber. Dorsal skin window chamber model (the diameter is 12 mm) is prepared when the mouse is in the state of anesthesia, injected with 100 μL phenobarbital solution [41].Complicated main vessels can be observed with naked eye. Dorsal skin window chamber model is shown as in Fig. 3. To make sure that the mouse model is in focus, we adjusted the height of the sample stage and obtained interference images simultaneously. At the same time, there is a proper angle between the sample and the horizontal plane to get suitable intensity from the reflected light.

Fig. 3 Dorsal skin window chamber model

The skin of human and higher animals is composed of cuticle, dermis and subcutaneous tissue. Dermis is located deep in the cuticle, the outermost layer of human and higher animals. There are abundant blood vessels, lymphatic vessels, nerves, sweat glands and hair follicles in the subcutaneous tissue (also called subcutaneous fat tissue). Capillaries produced by blood vessels cannot be seen with naked eyes due to their small size (6–9 μm). In view of calculated resolution, capillaries at these sizes can be obtained by this high-resolution SD-OCT system.

Figure 4 shows one set of representative OCT image and reconstructed 3D image of the skin of the mouse back. The

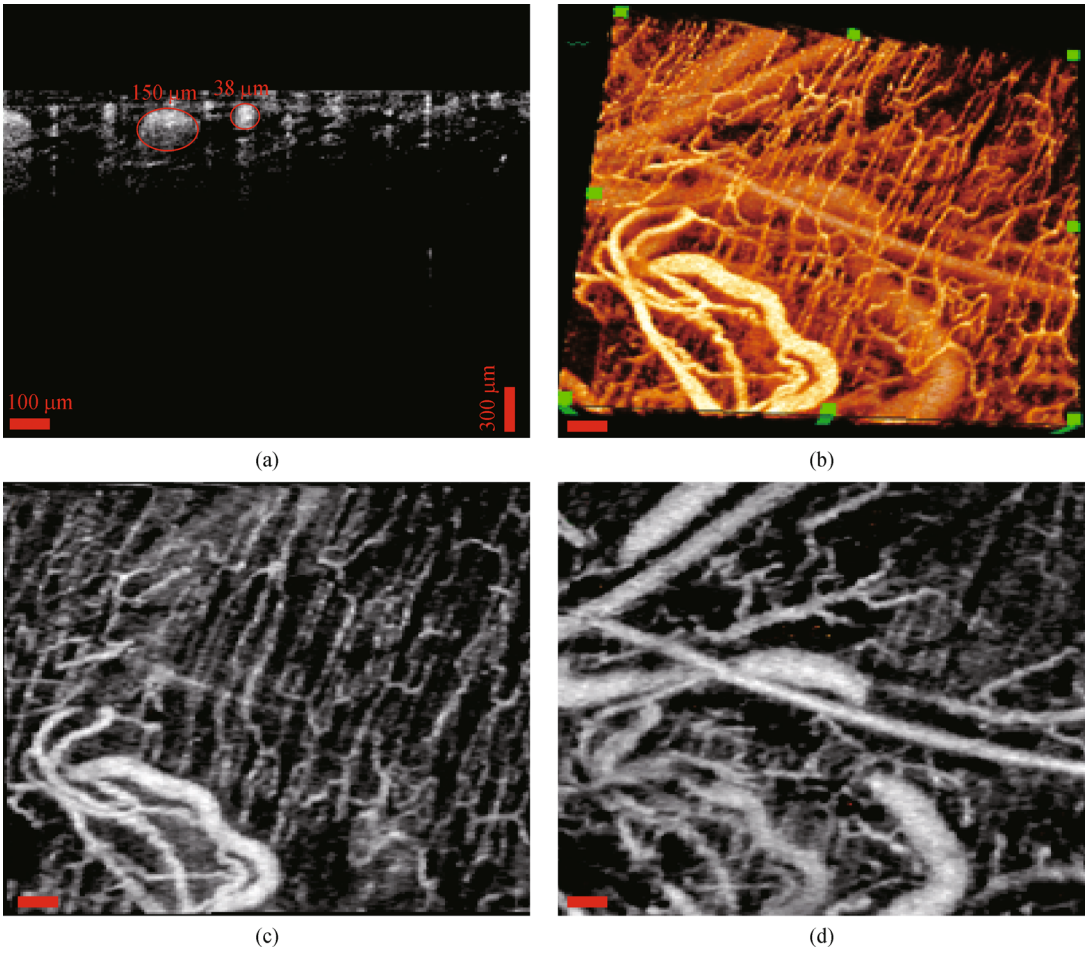

Fig. 4 Vascular distribution images of dorsal skin window chamber mouse model. (a) Real-time OCT image; (b) 3D image of the vascular distribution; (c) and (d) blood vessel distributions at two different depths, which are 80 and 320 μm, respectively. Scale bar in (a) is 300 μm in longitudinal direction, while the scale bar in transverse direction is 100 μm. Scale bars in (b), (c) and (d) are 100 μm

real-time cross-sectional image of blood vessels is shown in Fig. 4(a), indicating the size of blood vessels intuitively. Two blood vessels are marked with circles, and their diameters are 150 and 38 μm respectively. The imaging depth is about 610 μm. Reconstructed 3D image of the same position by Amira is shown in Fig. 4(b). Figures 4(c) and 4(d) show vascular distribution at two different depths. Vascular distributions at different layers of the mouse skin are different obviously. The size of the area in Fig. 4(a) (marked in red circle) corresponds to the diameter of the vessels in Figs. 4(b), 4(c) and 4(d).That is to say, the larger the size of the area forms, the bigger the diameter of the blood vessels is. Each image size is 1.3 mm ×1.3 mm.

4 Conclusion

A SD-OCT system has been developed to image the skin of the mouse *in vivo*. According to obtained OCT image and 3D image, complicated distribution of blood vessels exists in the deeper layer of the mouse skin. To our knowledge, this system can be further applied to observe vascular distribution of other tissues *in vivo*. The changes of vascular distribution of the mouse in different experiments can be visualized for a certain period of time. This system will provide a useful method for tumor research, e.g., to observe tumor growth or drug delivery in tumor therapy.

Acknowledgements This work was partially supported by the National Basic Research Program of China (No. 2015CB352005), the National Natural Science Foundation of China (Grant Nos. 61378091, 11204226, 11404285 and 61475143), Shenzhen Science and Technology Development Project (Nos. ZDSY20120612094247920, JCYJ20130329114905559 and CXB201104220021A), Zhejiang Provincial Natural Science Foundation of China (No. LY14F050007).

References

1. Huang D, Swanson E A, Lin C P, Schuman J S, Stinson W G, Chang

W, Hee M R, Flotte T, Gregory K, Puliafito C A, Fujimoto J G. Optical coherence tomography. Science, 1991, 254(5035): 1178–1181

2. Fujimoto J G, Brezinski M E, Tearney G J, Boppart S A, Bouma B, Hee M R, Southern J F, Swanson E A. Optical biopsy and imaging using optical coherence tomography. Nature Medicine, 1995, 1(9): 970–972
3. de Boer J F, Cense B, Park B H, Pierce M C, Tearney G J, Bouma B E. Improved signal-to-noise ratio in spectral-domain compared with time-domain optical coherence tomography. Optics Letters, 2003, 28(21): 2067–2069
4. Leitgeb R, Hitzenberger C, Fercher A. Performance of fourier domain vs. time domain optical coherence tomography. Optics Express, 2003, 11(8): 889–894
5. Choma M, Sarunic M, Yang C, Izatt J. Sensitivity advantage of swept source and Fourier domain optical coherence tomography. Optics Express, 2003, 11(18): 2183–2189
6. Fercher A F, Hitzenberger C K, Kamp G, El-Zaiat S Y. Measurement of intraocular distances by backscattering spectral interferometry. Optics Communications, 1995, 117(1–2): 43–48
7. Golubovic B, Bouma B E, Tearney G J, Fujimoto J G. Optical frequency-domain reflectometry using rapid wavelength tuning of a Cr^{4+}:forsterite laser. Optics Letters, 1997, 22(22): 1704–1706
8. Chinn S R, Swanson E A, Fujimoto J G. Optical coherence tomography using a frequency-tunable optical source. Optics Letters, 1997, 22(5): 340–342
9. Chen Z, Zhao Y, Srinivas S M, Nelson J S, Prakash N, Frostig R D. Optical Doppler tomography. IEEE Journal of Selected Topics in Quantum Electronics, 1999, 5(4): 1134–1142
10. Hee M R, Huang D, Swanson E A, Fujimoto J G. Polarization-sensitive low-coherence reflectometer for birefringence characterization and ranging. Journal of the Optical Society of America B, Optical Physics, 1992, 9(6): 903–908
11. Xu C, Ye J, Marks D L, Boppart S A. Near-infrared dyes as contrast-enhancing agents for spectroscopic optical coherence tomography. Optics Letters, 2004, 29(14): 1647–1649
12. Divetia A, Hsieh T, Zhang J, Chen Z, Bachman M, Li G. Dynamically focused optical coherence tomography for endoscopic applications. Applied Physics Letters, 2005, 86(10): 103902
13. Xiang S H, Chen Z, Zhao Y, Nelson J S. Multichannel signal detection of optical coherence tomography with different frequency bands. In: Proceedings of Conference on Lasers and Electro-Optics. 2000, 418
14. Rollins A M, Yazdanfar S, Barton J K, Izatt J A. Real-time *in vivo* color Doppler optical coherence tomography. Journal of Biomedical Optics, 2002, 7(1): 123–129
15. Wiesauer K, Pircher M, Götzinger E, Bauer S, Engelke R, Ahrens G, Grützner G, Hitzenberger C, Stifter D. En-face scanning optical coherence tomography with ultra-high resolution for material investigation. Optics Express, 2005, 13(3): 1015–1024
16. Feldchtein F, Gelikonov V, Iksanov R, Gelikonov G, Kuranov R, Sergeev A, Gladkova N, Ourutina M, Reitze D, Warren J. *In vivo* OCT imaging of hard and soft tissue of the oral cavity. Optics Express, 1998, 3(6): 239–250
17. Shao Y, He Y, Ma H, Wang S, Zhang Y. Study on mildew infecting skin of naked mouse by optical coherence tomography. Acta Laser Biology Sinica, 2006, 15(5): 536–539 (in Chinese)
18. Tomlins P H, Wang R K. Theory, developments and applications of optical coherence tomography. Journal of Physics D, Applied Physics, 2005, 38(15): 2519–2535
19. Swanson E A, Izatt J A, Hee M R, Huang D, Lin C P, Schuman J S, Puliafito C A, Fujimoto J G. *In vivo* retinal imaging by optical coherence tomography. Optics Letters, 1993, 18(21): 1864–1866
20. Zhao Y, Chen Z, Saxer C, Xiang S, de Boer J F, Nelson J S. Phase-resolved optical coherence tomography and optical Doppler tomography for imaging blood flow in human skin with fast scanning speed and high velocity sensitivity. Optics Letters, 2000, 25(2): 114–116
21. Zhao Y, Chen Z, Saxer C, Shen Q, Xiang S, de Boer J F, Nelson J S. Doppler standard deviation imaging for clinical monitoring of *in vivo* human skin blood flow. Optics Letters, 2000, 25(18): 1358–1360
22. Westphal V, Yazdanfar S, Rollins A M, Izatt J A. Real-time, high velocity-resolution color Doppler optical coherence tomography. Optics Letters, 2002, 27(1): 34–36
23. Yang V X D, Gordon M, Seng-Yue E, Lo S, Qi B, Pekar J, Mok A, Wilson B, Vitkin I. High speed, wide velocity dynamic range Doppler optical coherence tomography (Part II): imaging *in vivo* cardiac dynamics of Xenopus laevis. Optics Express, 2003, 11(14): 1650–1658
24. Ding Z, Zhao Y, Ren H, Nelson J, Chen Z. Real-time phase-resolved optical coherence tomography and optical Doppler tomography. Optics Express, 2002, 10(5): 236–245
25. Yazdanfar S, Rollins A M, Izatt J A. Imaging and velocimetry of the human retinal circulation with color Doppler optical coherence tomography. Optics Letters, 2000, 25(19): 1448–1450
26. Yazdanfar S, Rollins A M, Izatt J A.In vivo imaging of human retinal flow dynamics by color Doppler optical coherence tomography. Archives of Ophthalmology, 2003, 121(2): 235–239
27. Nassif N, Cense B, Park B H, Yun S H, Chen T C, Bouma B E, Tearney G J, de Boer J F. *In vivo* human retinal imaging by ultrahigh-speed spectral domain optical coherence tomography. Optics Letters, 2004, 29(5): 480–482
28. Leitgeb R, Schmetterer L, Drexler W, Fercher A, Zawadzki R, Bajraszewski T. Real-time assessment of retinal blood flow with ultrafast acquisition by color Doppler Fourier domain optical coherence tomography. Optics Express, 2003, 11(23): 3116–3121
29. White B, Pierce M, Nassif N, Cense B, Park B, Tearney G, Bouma B, Chen T, de Boer J. In vivo dynamic human retinal blood flow imaging using ultra-high-speed spectral domain optical coherence tomography. Optics Express, 2003, 11(25): 3490–3497
30. Chen T C, Cense B, Pierce M C, Nassif N, Park B H, Yun S H, White B R, Bouma B E, Tearney G J, de Boer J F. Spectral domain optical coherence tomography: ultra-high speed, ultra-high resolution ophthalmic imaging. Archives of Ophthalmology, 2005, 123 (12): 1715–1720
31. Makita S, Hong Y, Yamanari M, Yatagai T, Yasuno Y. Optical coherence angiography. Optics Express, 2006, 14(17): 7821–

7840
32. Wang R K, Jacques S L, Ma Z, Hurst S, Hanson S R, Gruber A. Three dimensional optical angiography. Optics Express, 2007, 15 (7): 4083–4097
33. Vakoc B J, Lanning R M, Tyrrell J A, Padera T P, Bartlett L A, Stylianopoulos T, Munn L L, Tearney G J, Fukumura D, Jain R K, Bouma B E. Three-dimensional microscopy of the tumor microenvironment in vivo using optical frequency domain imaging. Nature Medicine, 2009, 15(10): 1219–1223
34. Cardon S Z, Oestermeyer C F, Bloch E H. Effect of oxygen on cyclic red blood cell flow in unanesthetized mammalian striated muscle as determined by microscopy. Microvascular Research, 1970, 2(1): 67–76
35. Sandison J C. The transparent chamber of the rabbit's ear, giving a complete description of improved technic of construction and introduction, and general account of growth and behavior of living cells and tissues as seen with the microscope. American Journal of Anatomy, 1928, 41(3): 447–473
36. Laschke M W, Menger M D. *In vitro* and *in vivo* approaches to study angiogenesis in the pathophysiology and therapy of endometriosis. Human Reproduction Update, 2007, 13(4): 331–342
37. Yuan F, Chen Y, Dellian M, Safabakhsh N, Ferrara N, Jain R K. Time-dependent vascular regression and permeability changes in established human tumor Xenografts induced by an anti-vascular endothelial growth factor/vascular permeability factor antibody. Proceeding of the National Academy of Sciences, 1996, 93(25): 14765–14770
38. Huang D, Swanson E A, Lin C P, Schuman J S, Stinson W G, Chang W, Hee M R, Flotte T, Gregory K, Puliafito C A. Optical coherence tomography. Massachusetts Institute of Technology, Whitaker College of Health Sciences and Technology, 1993
39. Povazay B, Bizheva K, Unterhuber A, Hermann B, Sattmann H, Fercher A F, Drexler W, Apolonski A, Wadsworth W J, Knight J C, Russell P S, Vetterlein M, Scherzer E. Submicrometer axial resolution optical coherence tomography. Optics Letters, 2002, 27 (20): 1800–1802
40. Leitgeb R, Drexler W, Unterhuber A, Hermann B, Bajraszewski T, Le T, Stingl A, Fercher A. Ultrahigh resolution Fourier domain optical coherence tomography. Optics Express, 2004, 12(10): 2156–2165
41. Zhou J. Experimental observation on mice using dose phenobarbital sodium. Shanghai Laboratory Animal Science, 1988, 3: 139 (in Chinese)

Jian Gao received her B.S. degree in physics from Anqing Normal University, Anqing, China, in 2008. She is currently a third-year graduate student in the College of Optoelectronic Engineering in Shenzhen University. Her main research area is the applications of optical coherence tomography in biomedical imaging.

Xiao Peng received her Ph.D. degree from the Department of Applied Biology and Chemical Technology, Hong Kong Polytechnic University in 2007. She is currently a Lecturer in the College of Optoelectronic Engineering at Shenzhen University, and her research focuses on the application of optical techniques in biomedicine.

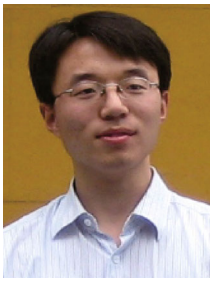

Peng Li is currently an Associate Professor of Optical Engineering at Zhejiang University. He received his B.E. degree in optoelectronic information engineering and Ph.D. degree in optical engineering from Nanjing University of Science and Technology in 2005 and 2010, respectively. After 3 years' postdoctoral research training at the University of Washington, Seattle, USA, he joined Zhejiang University in 2013. His current research interests include the development of non-invasive, high-resolution, high-speed optical biomedical imaging technology: optical coherence tomography (OCT), OCT-based angiography, OCT-based elastography, laser speckle, photoacoustic imaging, and their applications in neurology, ophthalmology, dermatology and tumor. He has published more than 20 peer-reviewed SCI journal articles and more than 10 international conference papers. The significance of his work is further emphasized by peer selection of his article for a special SPIE recommendation.

Zhihua Ding received his B.E. from Department of Optical Engineering at Zhejiang University (1989) and Ph.D. degree from Shanghai Institute of Optics and Fine Mechanics in China (1996). He was a Temporary Lecturer at Venture Business Laboratory of Shizuoka University in Japan (1998–2000) and a Senior Postdoctoral Fellow at Beckman Laser Institute of University of California at Irvine (2000–2002). From 2002, he joined the Department of Optical Engineering at Zhejiang University. He was enrolled as a member of New Century Excellent Talents in University (2004). He is an editorial board member of "*Journal of Lasers, Optics & Photonics*", "*Frontiers of Optoelectronics*", "*Journal of Innovative Optical Health Sciences"*, an associated editor of "*Acta Laser Biology Sinica*", and an executive member of the editorial board for "*Chinese Journal of Lasers*" . His research aims to investigate light/tissue (cell) interactions at micro to nano scale for high resolution and novel contrast, develop optical instruments for biomedical applications and fundamental researches. His current research foci are *in vivo* optical imaging and other *in vitro* optical methods, especially in optical coherence tomography.

Junle Qu received his Ph.D. degree in 1998 from Xi'an Institute of Optics and Precision Mechanics, Chinese Academy of Sciences. He is currently a Professor in the College of Optoelectronic Engineering at Shenzhen University, and his research field includes fluorescence lifetime imaging microscopy, super-resoution optical imaging and their applications in biomedicine.

Hanben Niu graduated from the Department of Radio-electronics at Tsinghua University in 1966. He is currently an Academician of the Chinese Academy of Engineering, and a Professor in the College of Optoelectronic Engineering at Shenzhen University. His research field includes super-resolution fluorescence imaging, X-ray phase contrast imaging and ultrafast phenomenon diagnosis.